MATERIAL CONSTANTS OF AN Al-Li-Cu-Mg-Zr ALLOY DURING DEFORMATION AT ELEVATED TEMPERATURES①

Shen Jian

General Research Institute for Non-ferrous Metals, Beijing 100088, P. R. China

ABSTRACT The hot deformation behaviors of an 2091 Al-Li-Cu-Mg-Zr alloy have been investigated by high temperature isothermal compression testing. The material constants of the alloy, including deformation activation energy ΔH as 162.5 kJ/mol, stress-level coefficient α as 0.0397 mm^2/N, stress exponential n as 2.647 and structural factor A as 2.74×10^{10} s^{-1} are derived by both graphic representation method and minimized deviation criterion from the interdependencies of flow stress, strain rate and temperature. That the deformation activation energy of the 2091 alloy is higher than the self-diffusion activation energy of pure aluminium for high temperature creep and the activation energy of most other commercial aluminium alloys can be attributed to the alloying of copper and magnesium.

Key words aluminium-lithium alloy compression flow stress activation energy

1 INTRODUCTION

It is generally accepted that many hot-working processes are thermally activated, where operating deformation mechanisms are an extension of the deformation mechanism in creep under different stress levels, and that Garofalo's equation relating steady-creep strain rate, temperature and flow stress may be applied generally to these processes.

A number of evidences[1-3] about the high temperature deformation and conventional hot-working processes of different metals and materials suggested that the power law and the exponential relationship correlate strain rate $\dot{\varepsilon}$ with steady state flow stress σ of the materials at low and high stress levels as follows, respectively

low stress: $\dot{\varepsilon} = A_1\sigma^{n_1}$ (1)

high stress: $\dot{\varepsilon} = A_2\exp(\beta\sigma)$ (2)

where n_1 and β are temperature-independent constants. When investigating the experimental stress-strain relationship of steel under quick tension, Zener and Hollomon[4] found a parameter of so-called "temperature-compensated strain rate", i.e. Z parameter, correlating flow stress to deformation variables as

$$Z = A[\sinh(\alpha\sigma)]^n = \dot{\varepsilon}\exp\left(\frac{\Delta H}{RT}\right) \quad (3)$$

where A is structural factor; n, α and ΔH is stress exponential, stress-level coefficient and deformation activation energy, respectively; R is universal gas constant and T is the absolute temperature. The eqn. (3) has shown good agreement with many experimental data within wide strain rate and temperature ranges[1].

Compared with eqns. (1) to (3), it can be concluded that eqn. (3) approximates a power relation, eqn. (1), at low stress; and an exponential relation, eqn. (2), at high stress. Many researches proved that this relationship could describe well the conventional hot-working processes, such as extrusion, compression and torsion[1,2]. Thus, after evaluating the material constants of A, n, α and ΔH etc., eqn. (3) may be utilized to the prediction, control and optimization of the microstructures and properties of the hot-deformed metals and alloys from the relationships between flow stress and processing

① Received Apr. 15, 1997; accepted Jul. 11, 1997

variables and further between flow stress and structural information.

2 PRINCIPLE

Many approaches are suitable for material constants determination, including isothermal-, time-compensation, temperature-alternation and Zener-Hollomon methods, the last one is generally used in rate-controlling deformation, and is under present consideration.

In creep testing, since a constant stress can be applied over a range of temperatures, the creep activation energy ΔH can be calculated from a plot of $\ln\dot{\varepsilon}_s$ at constant σ as a function of the reciprocal of the temperature, which is proportional to ΔH[5]. In hot compression tests, however, since it is experimentally much more difficult to conduct tests at constant flow stress over large strain, a constant strain rate is applied and the resultant stress is measured. The calculation of ΔH at constant stress therefore involves extensive extrapolation and interpolation of the experimental stress-strain rate-temperature data.

Flow stress of the material satisfies the relationships identified by eqns. (1) and (2) with strain rate for different stresses. The constants in eqn. (1) and eqn. (2) can then be derived from the corresponding values $\ln\dot{\varepsilon}$ vs $\ln\sigma$ for low stress and the corresponding values $\ln\dot{\varepsilon}$ vs σ for high stress. Then the material constants, A, n and α can be obtained from the experimental data according to a wide range of strain rates and temperatures

$$\begin{cases} n = n_1 \\ \alpha = \beta / n \\ A = A_1 2^n \end{cases} \tag{4}$$

These material constants, however, must be a first approximation because relatively few experimental points have been used in each calculation. The activation energy ΔH should be evaluated before the calculation of the valid constants.

For small values of α and low applied stress, as in the case of aluminium and its alloys, the eqn. (3) reduces to

$$\dot{\varepsilon} = A\sigma^n \exp(\frac{\Delta H}{RT}) \tag{5}$$

Partial differentiation of eqn. (5) gives

$$\Delta H = R \cdot \left| \frac{\partial \ln\dot{\varepsilon}}{\partial \ln\sigma} \right|_T \cdot \left| \frac{\partial \ln\sigma}{\partial(1/T)} \right|_{\dot{\varepsilon}} \tag{6}$$

The activation energy is calculated using eqn. (6) and by plotting $\ln\dot{\varepsilon}$ as a function of $\ln\sigma$ and $\ln\dot{\varepsilon}$ as a function of σ at any selected temperature and strain rate.

For 2091 Al-Li alloy, since the flow stress-strain rate-temperature interrelationship fits hyperbolic sine relationship more than logarithms term[6], it is more reasonable to use stress term of $\sinh(\alpha\sigma)$ instead of σ. This leads to a satisfactory correlation that enables the unambiguous determination activation energy of the 2091 Al-Li alloy from the following modified equation

$$\Delta H = R \cdot \left| \frac{\partial \ln\dot{\varepsilon}}{\partial \ln\sinh(\alpha\sigma)} \right|_T \cdot \left| \frac{\partial \ln\sinh(\alpha\sigma)}{\partial(1/T)} \right|_{\dot{\varepsilon}} \tag{7}$$

where the last two terms of eqn. (7) represent the slope of the $\ln\dot{\varepsilon}/\ln[\sinh(\alpha\sigma)]$ plot at the temperatures employed and the slope of $\ln[\sinh(\alpha\sigma)]/(1/T)$ at the strain rates of interest, respectively.

3 EXPERIMENTAL PROCEDURE

The tested 2091 Al-Li alloy with the composition of Al-2.06Li-2.22Cu-1.48Mg-0.097Zr-0.17Fe-0.08Si was prepared by conventional IM method. Solid cylinder upsetting Rastegaev specimens, with flat recesses in the both ends, with the gauge dimension of 10 mm in diameter and 15 mm in length were machined from the 524 ℃/24 h homogenized ingots. The constant-strain rate compression test was carried out at elevated temperatures using a Gleeble 1500 dynamic material testing machine with two polished tungsten platens. The strain rate and the temperatures of interest are within the range of 300~500 ℃ and 10^{-3}~10^{1} s^{-1}, respectively. The deformation variables, such as stroke, stroke velocity and temperature, were controlled, and the data of true stress, true stain and load, etc, were recorded by the computer of the apparatus. The homogeneous flow stress was derived out from the experimental data considering friction modification[6].

4 RESULTS AND DISCUSSION

The homogeneous flow stress of the 2091 Al-Li alloy after friction modification is shown in Table 1. The material constants are evaluated from the experimental data of flow stress, strain rate and temperature.

Table 1 Friction modified flow stress σ of tested 2091 Al-Li alloy at different temperatures(MPa)

$\dot{\varepsilon}/s^{-1}$	300 ℃	350 ℃	400 ℃	450 ℃	500 ℃
0.001	79.5	42.1	22.9	18.4	5.9
0.01	101.4	63.1	39.5	26.8	14.2
0.1	128.7	90.0	62.6	43.3	30.9
1.0	148.2	111.9	81.7	58.4	43.0
10.0	158.9	132.2	104.2	82.8	68.4

The alternation of the flow stresses of the 2091 alloy during hot compression with strain rates and temperatures are shown in Fig. 1 and Fig. 2, which are plotted on a semi-ln basis and a ln-ln basis with respect to temperature and strain rate, respectively. The plots of either the natural logarithms of hyperbolic of flow stresses against the reciprocals of the corresponding temperatures (in Fig. 1) or the natural logarithms of strain rates against the hyperbolic of flow stresses (in Fig. 2) satisfy straight line relationships over the experimental data, indicating that the hot compression of the 2091 alloy is thermally activated, thereby supporting the Arrhenius dependence similar to eqn. (3).

The average slopes of the straight lines in both Fig. 1 and Fig. 2 were calculated by linear regression with a FORTRAN 77 computer program, and the results are substituted in eqn. (6) to evaluate the activation energy (as be termed as graphic representation method). After the activation energy derived, it is possible to calculate the temperature-compensated strain rate from eqn. (3) and the refined values of n and α may be obtained from the relationships such as shown in eqn. (3) and eqn. (4). Thereafter the second value of ΔH can be calculated from eqn. (7). The values of n and α must be compatible such that the minimum standard deviation of n is obtained over the hot compression range. Hence, a considerable amount of iteration is necessary to evaluate valid material constants, according to

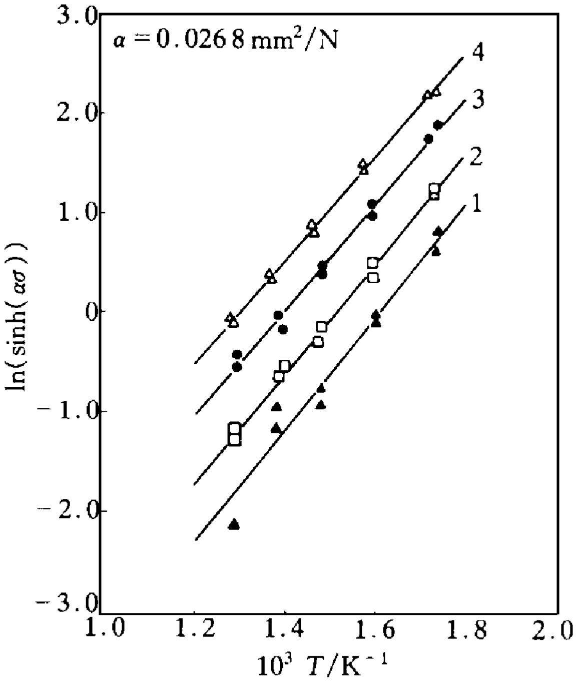

Fig. 1 Temperature dependence of flow stress of tested 2091 alloy

1 — $\dot{\varepsilon}$ = 0.001 s^{-1}; 2 — $\dot{\varepsilon}$ = 0.1 s^{-1};
3 — $\dot{\varepsilon}$ = 0.01 s^{-1}; 4 — $\dot{\varepsilon}$ = 1.0 s^{-1}

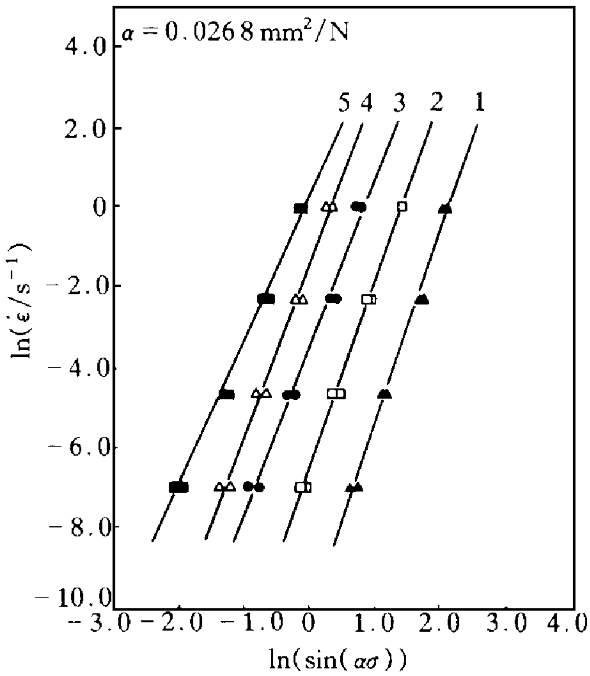

Fig. 2 Interdependencies of flow stress and strain rate of tested 2091 alloy

1 — t = 300 ℃; 2 — t = 350 ℃;
3 — t = 400 ℃; 4 — t = 450 ℃; 5 — t = 500 ℃

the minimized deviation method[7].

The material constants evaluated by the aforementioned methods are listed in Table 2.

Table 2 The materials constants of the 2091 alloy evaluated by differrent method

Method	Activation Energy ΔH / kJ·mol	Stress-level coefficient α/ mm^2·N	Stress exponential n	Strucutral factor A / s^{-1}
Graphic representation	154.5	0.0268	2.809	2.17×10^{10}
Minimized deviation	162.5	0.0397	2.647	2.74×10^{10}

The logarithms of temperature-compensated strain rate Z parameter against sinh($\alpha\sigma$) calculated from the constants, which have been evaluated by the minimized deviation method, is illustrated in Fig. 3. The plot gives good agreement of ln$Z$ with lnsinh($\alpha\sigma$) in the linear relationship over the strain rate and temperature ranges of interest, indicating that the hot compression of the 2091 alloy involves the thermally activated rate-controlling mechanisms, and permitting the effective prediction, control and optimization of the hot-deformed microstructures and properties of the alloy with the aim of Z parameter containing Arrhenius term.

The deformation activation energy of the 2091 alloy (162.5 kJ/mol) is somewhat higher not only than the self-diffusion activation enthalpy of pure aluminium (142 kJ/mol) but also than that of most other commercial aluminium alloys[1,2]. This might be attributed to the addition of the elements of copper and magnesium and so on, as discussed afterwards.

The addition of copper and magnesium to the Al-Li alloy gives solution strengthening effect to the 2091 alloy and forms precipitation, such as $CuAl_2$, Al_2MgLi and Al_2CuMg, within the matrix. The precipitation retards the movement of dislocations during plastic deformation, resulting in the increase of energy needed for dislocations to slip and/or to climb and thus the difficulty to activate dynamic recovery. Furthermore, on one hand the formation of Al_3Zr precipitation in the 2091 alloy strongly impedes the movement of dislocations, grain- and subgrain boundaries[6], hence increases the softening energy of the alloy to a considerable extent. On the other hand, the fine second phase particles, such as δ', θ and S, which have been precipitated during the reheating process before hot-working may remelt into the solution during hot deformation. The activation energy may then rise when the fine precipitation goes into the solution[7].

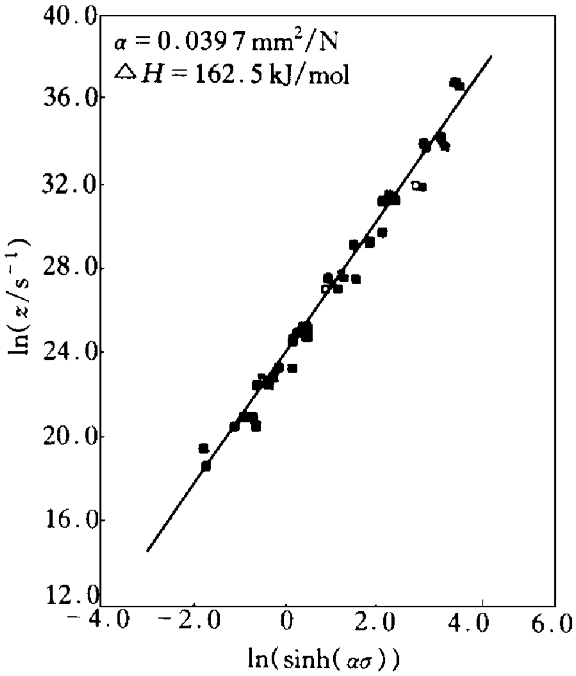

Fig. 3 Linear relationship of ln$Z$ vs ln[sinh($\alpha\sigma$)] for 2091 alloy

Eqn. (3) and eqn. (5), however, are not based on any theoretical model or atomistic rate-controlling mechanism and the constants A, α and n do not have simple physical interpretations. A more rigorous equation suggested by Seeger[8], later modified by Jonas[9] has been found very useful:

$$\dot{\varepsilon}_s = \varphi_s \exp\left(\frac{-\Delta H_0}{kT}\right)\exp\left(\frac{V^*\sigma^*}{kT}\right) \qquad (8)$$

where $\dot{\varepsilon}_s$ is the steady-state strain rate, φ_s is a structure factor involving dislocation density and area slipped and Burgers' vector and atomic frequency as well ΔH_0 is the activation enthalpy at zero stress, V^* is the activation volume, σ^* is the effective stress ($\sigma^* = \sigma_A + \sigma_B$, where σ_A is the applied stress, and σ_B is the back-stress[10]), k is the Boltzmann constant and T is the absolute temperature. Eqn. (8) indicates the physical essence of high temperature deformation of the materials.

Experimental values of ΔH are usually calculated by assuming that the structure depends on the steady-state stress alone, and it is independent of temperature. The partial differentiation of eqn. (8) to ($1/T$) gives

$$\left(\frac{\partial \ln \dot{\varepsilon}_s}{\partial(1/T)}\right)_{\sigma^*} = \frac{-\Delta H}{k} + \left(\frac{\partial \ln \varphi_s}{\partial(1/T)}\right)_{\sigma^*} + \frac{\sigma^*}{k}\left[V^* + \left(\frac{\partial V^*}{\partial \ln(1/T)}\right)_{\sigma^*}\right] \quad (9)$$

The creep activation energy can be obtained from eqn. (9) when the two terms following ($\Delta H/k$) on the right of the equation are neglected. These assumptions are not always valid and the two terms are not negligible, however, especially with regard to certain solid-solution alloys during hot-working[1]. The activation volume V^* and back-stress σ_B of the alloy may be changed by solid-solution alloying, resulting in the variation of apparent activation energy V($V = V^*/M_T$, where M_T is effective Tablor orientation factor and effective stress and finally the variation of the activation energy ΔH. The alloying of Cu and Mg raises the back-stress, σ_B, of the 2091 alloy, hence reduces the effective stress. Higher applied stress must be supplied to the alloy during hot deformation to maintain the constant strain rate, thus leading to the rise of the activation energy.

5 CONCLUSIONS

(1) Straight line relationship can be found to satisfy either the natural logarithms of strain rate to the hyperbolic form of the flow stress or hyperbolic form of the natural logarithm of the flow stress to the reciprocal of the temperature for the 2091 Al-Li alloy during hot compression.

(2) Both the graphic representation method and the minimized deviation criterion have been conducted to evaluate the material constants of the 2091 alloy. The constant derived from the minimized deviation criterion are as follows:

Activation energy ΔH, 162.5 kJ/mol;

Stress-level coefficient α, 0.0397 mm^2/N;

Stress exponential n, 2.647;

Structure factor A, $2.74 \times 10^{10}\ s^{-1}$.

(3) The reason that higher activation energy of the 2091 alloy during hot deformation than self-diffusion activation enthalpy of the commercial pure aluminium can be attributed to the alloying of copper and magnesium into the matrix.

REFERENCES

1 Jonas J J, Sellars C M and McG Tegart W J. Int Metall Rev, 1969, 130(14): 1.

2 Poirier J P ed. Plastic Deformation of the Crystals at Elevated Temperatures, (in Chinese). Dalian: Dalian University of Science and Technology Press, 1989: 24.

3 Jonas J J, McQueen H J and Wong W A. Deformation under Hot Working Conditions. London: Iron and Steel Institute, 1968: 49.

4 Zener C, Hollomon J H. J Appl Phys, 1944, 15(1): 22.

5 Wong W A, Jonas J J. Trans Metall Soc AIME, 1968, 242(11): 2271.

6 Shen Jian. PhD Dissertation, (in Chinese). Changsha: Central South University of Technology, 1996: 19.

7 Raybould D, Sheppard T. J Inst Metals, 1973, 101: 65.

8 Seeger A. Phil Mag, 1955, 46: 1194.

9 Jonas J J. Acta Metall, 1969, 17: 397.

10 Jonas J J. Acta Metall, 1969, 17(4): 397.

(Edited by Huang Jinsong)